

Chapter 13

535 kV/25 kA Hybrid Circuit Breaker Development



Zhanqing Yu, Rong Zeng, Lu Qu, Yulong Huang, Xin Yan, Zhizheng Gan, Xiangyu Zhang, and Zhengyu Chen

1 Introduction

This section will focus on the development of the 535 kV hybrid DC circuit breaker for the Zhangbei flexible DC transmission project [1, 2], the world's first HVDC grid, based on the 535 kV hybrid circuit breaker topology proposed by Tsinghua University [3]. This chapter will give the development process of the ultrafast mechanical switch (MS) [4], the modular-designed high-current bidirectional solid-state switch (SS) [5, 6], the current commutation driver circuit (CCDC) [7], and the isolation energy supply system [8]. Finally, 25 kA breaking experiment and reclosing experiment of the 535 kV circuit breaker are designed and carried out.

There are three main technical approaches to realize the fault isolation and protection of DC side based on protection equipment: (1) AC circuit breaker, (2) adopt converter with self-clearing capability of DC side fault, and (3) DC circuit breaker. Among them, the DC circuit breaker plays an important role in closing, carrying, and breaking the current under normal circuit conditions, converting the operating mode of the system, and breaking the fault current to protect the system. It is the preferred solution to realize the fault handling of the DC power grid.

According to the topology and breaking principle, DC circuit breakers can be divided into mechanical DC circuit breakers, solid-state DC circuit breakers, and hybrid DC circuit breakers. Among them, the mechanical DC circuit breaker has low conduction loss, but its breaking speed is relatively slow, and the breaking dispersion is high. The solid-state DC circuit breaker has an extremely fast breaking speed, but its on-state loss is large, and the cost is high. The hybrid DC circuit breaker combines the advantages of mechanical DC circuit breakers and solid-

Z. Yu (✉) · R. Zeng · L. Qu · Y. Huang · X. Yan · Z. Gan · X. Zhang · Z. Chen
Tsinghua University, Beijing, China
e-mail: yzq@tsinghua.edu.cn

state DC circuit breakers and has the advantages of strong controllability and fast reclosing, which can meet the needs of flexible DC power grid fault protection, so it has become one of the main development directions of DC circuit breakers.

Reliable and fast current transfer is a prerequisite for the successful current interruption of hybrid DC circuit breakers. According to the principle of current transfer, the commutation modes of hybrid DC circuit breakers can be divided into natural commutation type, voltage zero-crossing type, and resistance zero-crossing type. The hybrid DC circuit breaker based on the natural commutation has the advantages of small on-state loss, fast breaking speed, etc. However, this commutation method is limited by the mechanical switching arc voltage. With the increase of the voltage level of the DC circuit breaker, the number of devices required in series in the power electronic switch branch increases, and the on-state voltage drop of the transfer branch increases. To ensure that the current is fully diverted to the power electronics branch, higher voltages will be required, placing higher demands on the switches and the power electronics branch. In the hybrid DC circuit breaker based on resistance zero-crossing, since the main power electronic switch conducts current for a short time and the conduction loss is very low, it is not necessary to install a cooling system. However, the auxiliary power electronic switch passes through the rated current for a long time, and the on-state loss is tens of kilowatts, which requires a water-cooled heat dissipation system, increasing the complexity and maintenance cost of the system. Tsinghua University proposed a voltage zero-crossing hybrid DC circuit breaker based on the coupled negative voltage circuit. The coupled negative voltage circuit can ensure the fast and reliable transfer of bidirectional current without increasing the on-state loss of the DC circuit breaker. The main circuit has only mechanical switches, no additional cooling device required. Compared with other methods, this topology has the advantages of simple structure, reliable commutation, and suitable for any voltage level (Fig. 13.1).

2 535 kV Coupling Negative Voltage Commutation Hybrid DC Circuit Breaker Overall Design

The hybrid DC circuit breaker is the same as most hybrid DC circuit breakers, with three branches: an ultrafast mechanical MOV switch, a bidirectional solid-state switch module, and an energy-consuming MOV [9, 10]. The circuit breaker topology and breaking process are shown in Fig. 13.2. In addition, a current commutation driver circuit that can actively generate a pulse voltage is connected in series with modular solid-state switches to replace the load commutation switch on the mechanical switch branch. This allows the load current to flow only through the mechanical switch without other loss when the circuit breaker is normally operated [11]. When a short-circuit fault occurs, the mechanical switch starts to open, generating an arc. At the same time, the modular solid-state switches will be turned on, and CCDC

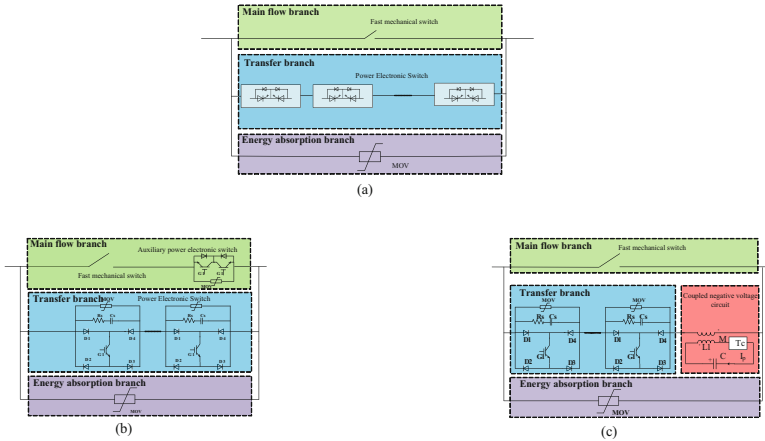


Fig. 13.1 Hybrid DC circuit breaker topology comparison. (a) Natural commutation hybrid DC circuit breaker topology. (b) Resistor zero-crossing hybrid DC circuit breaker topology. (c) Voltage zero-crossing hybrid DC circuit breaker based on coupled negative voltage

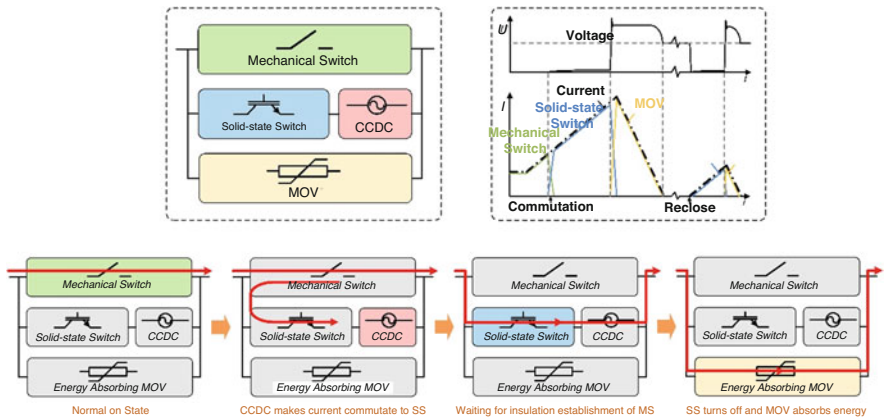


Fig. 13.2 The interruption process of the proposed HCB

generates a pulsed voltage and drives the fault current to commute from the mechanical switch to the solid-state branch. The voltage generated by the CCDC is alternating. So, bidirectional commutation of the circuit breaker can be achieved. The arc in mechanical switch is extinguished when the current crosses zero, while solid-state switches continue to carry current until the mechanical switch contacts are pulled apart far enough to withstand the overvoltage. Finally, the solid-state switches are turned off, and the energy-consuming MOV will absorb the remaining energy [12, 13]. In addition, the reclosing function can be easily realized by using the solid-state switches. The CCDC can be regarded as a small inductance of 100 μ H

Table 13.1 Main parameter requirements of 535 kV circuit breaker

Index	Parameters
Rated voltage	535 kV
Rated current	3300 A
Breaking capability	25 kA
MOV residual voltage	800 kV
Breaking speed	<3 ms

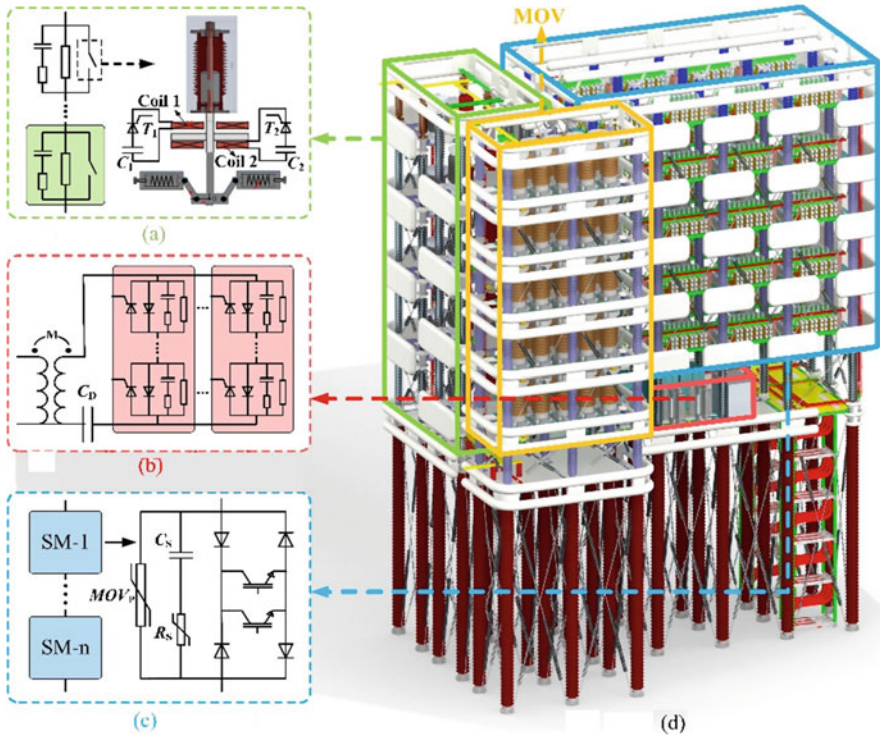


Fig. 13.3 Design of key components of coupling negative voltage hybrid DC circuit breaker. (a) Mechanical switch. (b) Coupling negative voltage device. (c) Solid-state switch. (d) Structure

when it does not work, which will have no significant impact on the solid-state switches.

According to the system requirements, the main parameters proposed for the DC circuit breaker are shown in Table 13.1. The following will introduce the design of the 535 kV hybrid DC circuit breaker in detail, as shown in Fig. 13.3, including design of mechanical switch for rapid breaking and restoration, modular-designed high-current bidirectional solid-state switch, and design of reliable CCDC.

3 Ultrafast Mechanical Switching of DC Circuit Breakers

The breaking time of the hybrid circuit breaker mainly depends on the speed of the mechanical switch. The solid-state switches can be turned off when the contact distance of the mechanical switch can withstand the overvoltage. Therefore, the moving contact must be separated to a certain distance as quickly as possible [14]. The bidirectional Thomson-coil actuator, which can accelerate and decelerate the moving parts, is developed to achieve this goal. As shown in Fig. 13.4, to achieve a better arc recovery effect, the ultrafast mechanical switch adopts a vacuum interrupter that the moving contact is connected to a metal disk placed between the two coils. In the closed state, the metal disc is close to the coil 1. When the precharged capacitor C_1 discharges through thyristor T_1 to coil 1, the metal disk, which is connected to the moving contact, will be forced to move away from coil 1. Then, after several milliseconds, the precharged capacitor C_2 discharges through thyristor T_2 to coil 2 to decelerate the metal disk and avoid the heavy bounce when the moving parts reach the other side. In addition, the switch also uses a bistable spring mechanism as a holding unit, so that the moving and static contacts can be closely contacted to ensure a sufficiently small contact resistance during normal flow.

Typical moving curves for ultrafast mechanical switch opening are given in Fig. 13.5. It can be seen that the electromagnetic repulsion mechanism can pull the switch contacts apart by a distance of 15 mm within 3 ms, which can withstand 160 kV operating overvoltage. Under the buffer action of coil 2, the speed of the moving parts is reduced to fewer than 1 m/s to protect the mechanical structure.

The overall mechanical switch branch consists of eight ultrafast mechanical switches connected in series. Figure 13.6 shows the comparison of the moving curves of eight ultrafast mechanical switches. Within the initial movement of about 15 mm, the switches are relatively consistent. But when the coil 2 starts to buffer, the movement of switches is different obviously because of the mechanical properties of the switches. During the breaking process of the circuit breaker, only the action characteristics of the mechanical switch in the first 3 ms are concerned. The total

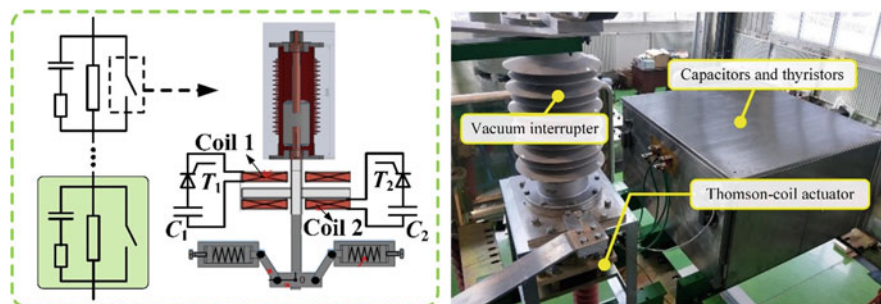


Fig. 13.4 Principle and physical map of fast mechanical switch

Fig. 13.5 Typical switch travel curve

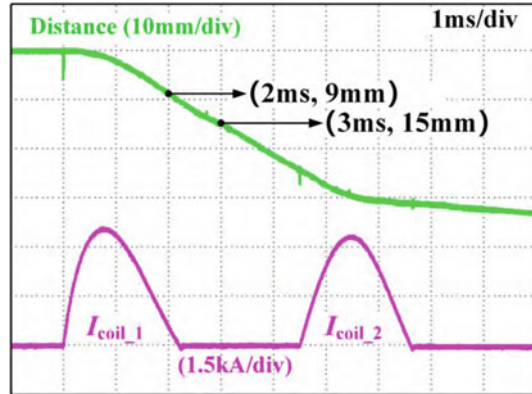
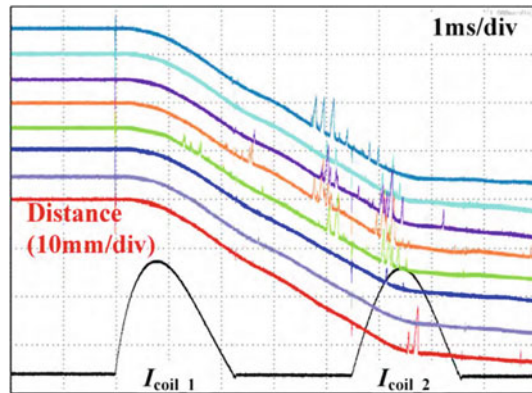


Fig. 13.6 Comparison of eight switch moving curves



opening distance of eight mechanical switches can reach more than 96 mm in 2 ms, which is enough to withstand the 800 kV overvoltage. In addition, in order to avoid uneven voltage between switches, each switch is also connected in parallel with a static voltage equalization resistor (300 M Ω) and a dynamic voltage equalization RC circuit (300 Ω , 5 nF).

4 Design and Development of 535 kV/25 kA Solid-State Switches

The modular-designed high-current bidirectional solid-state switch is the core component of the hybrid DC circuit breaker. It not only needs to have a surge capacity to withstand millisecond-level fault currents but also a cutoff capability of up to 25 kA. In addition, as part of the 500 kV HCB, it must withstand the rated voltage and transient overvoltage. To ensure the reliability of the solid-state branch, this project requires at least two parallel full-control devices in a solid-state switch

module. In this way, the two parallel devices are bypass switches for each other to avoid the failure of current commutation caused by the refusal of a single device (such as driving optical fiber, poor lead contact, etc.).

4.1 Selection of Power Electronic Devices

In the application of hybrid high-voltage DC circuit breakers, IGBT-type devices with strong current shutoff capability usually are used as full-control devices for solid-state switches [15]. Considering the device characteristics, prices, and application reliability, Toshiba’s 4.5 kV/3 kA IEGT (ST3000GXH24A) was finally selected [16]. IEGT is a kind of IGBT that uses an enhanced injection structure with a low on-state voltage, making it ideal for use in DC circuit breakers that require high-current capability. The effect of the enhanced injection structure makes the internal current distribution closer to the IGCT when the device is turned on. So the desaturation current of IEGT will be greatly improved after the gate voltage is increased. Figure 13.7 shows the result of the turnoff capability test of IEGT. In Fig. 13.7a, it can be seen that the device has obvious desaturation at about 10.4 kA with

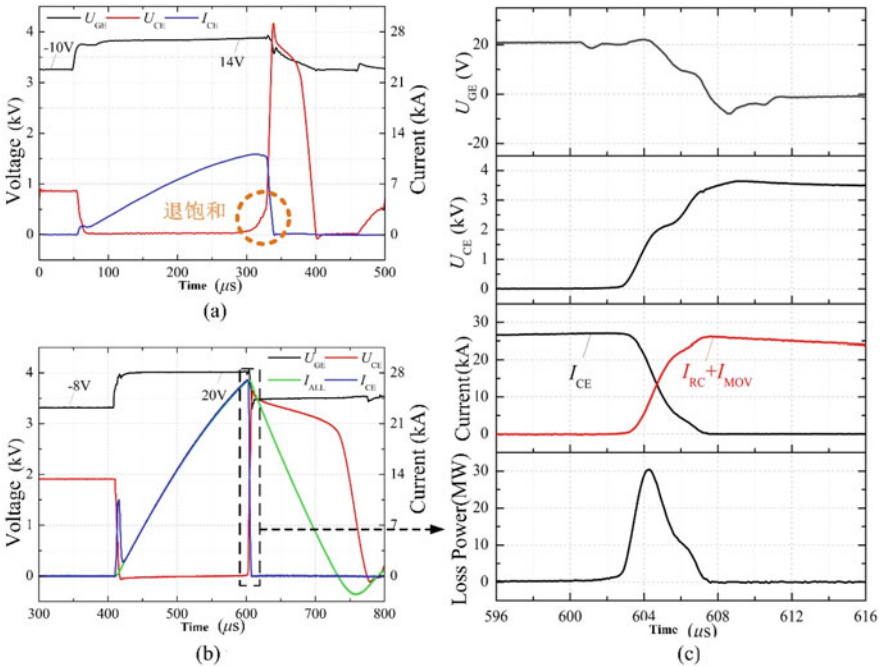


Fig. 13.7 IEGT turnoff performance test. (a) Desaturation of IEGT at 10.4 kA. (b) The waveform of breaking 27 kA current. (c) The detail of breaking 27 kA current

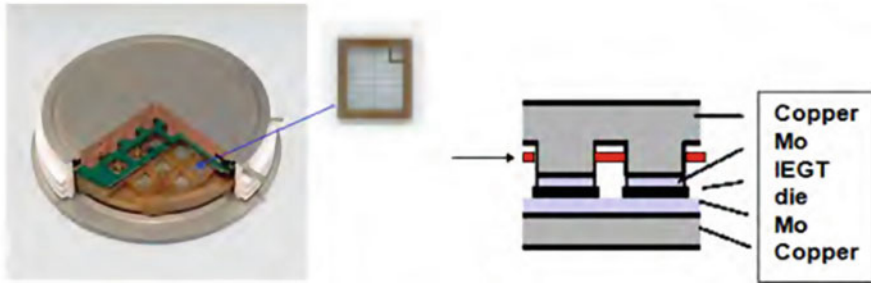


Fig. 13.8 IEGT in press-fit package

14 V gate voltage. Because it is turned off after a short time, IEGT is not damaged when breaking 10.4 kA current. When the gate voltage is increased to 20 V (Fig. 13.7b), the current reaches 27 kA without desaturation, and it is successfully turned off. As is shown in Fig. 13.7c, the transient power loss that the IEGT can withstand when turned off can reach 30 MW, which is enough to meet the requirement of Zhangbei Project for the turnoff capability of IEGT.

Because IEGT is a double-sided crimp construction (Fig. 13.8), there is no bonding line inside. In this configuration, the silicon chip is sandwiched between the molybdenum material and the copper for the outer packaging. When a short-circuit fault occurs, the metal alloy material formed after melting can ensure long-term reliable flow, which is called long-term failure short-circuit mode. In this way, when IEGT in the module fails, it can maintain a short-circuit state by itself and have no influence on other modules, improving the reliability of equipment.

Because of the optimization of the diode bridge structure, a standard recovery diode with low cost and strong surge capability can be used to form a bidirectional structure. The diode was selected as Infineon D1800N48T (4800 V 1800 A). Because the conduction voltage drop of standard recovery diode is very low, the surge capability in 3 ms of this diode can exceed than 35 kA.

4.2 Structural Design and Optimization

The module structure needs to be as compact as possible to reduce the impact of stray inductance on the commutation process, as shown in Fig. 13.9. First, to achieve consistency of parallel IEGT in a module, two IEGTs are symmetrically pressed, and the cathodes of them share the same heat sink. Then four diodes are individually press-fitted in another valve section to avoid the mutual influence with IEGT valve. Besides, snubber circuit and MOV are symmetrically placed on the outside of the diode bridge to realize the bidirectional current flow. All connecting copper bars need to be placed as close as possible to reduce the effect of stray inductance on the breaking process.

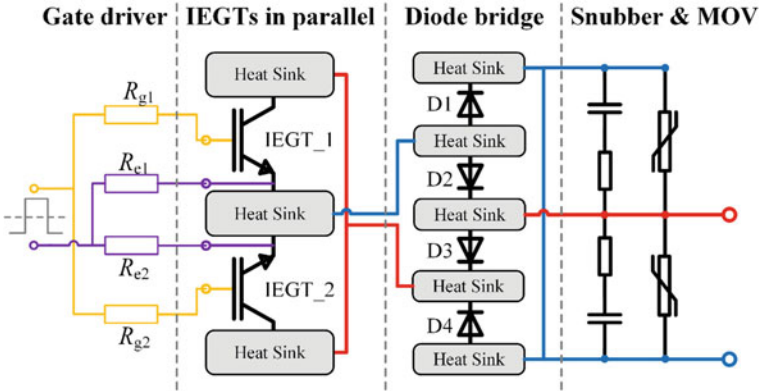
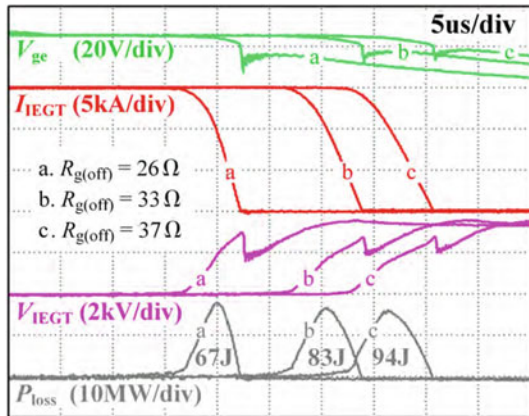


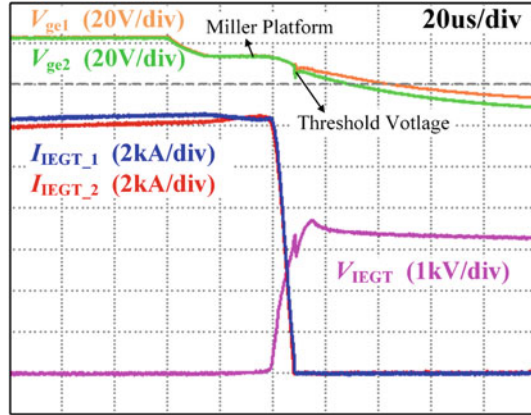
Fig. 13.9 Schematic diagram of the parallel structure of power electronic multilevel direct-series switches

Fig. 13.10 Gate resistor adjustment



The gates of the parallel IEGTs are connected to the output port of the driver through two independent gate resistors ($R_{g1} = R_{g2} = 33 \Omega$) which are the same in resistance. Two cathode resistors are also added to suppress the circulating current caused by the asymmetry of the driver connection line ($R_{e1} = R_{e2} = 1 \Omega$). The gate resistance affects the turnoff speed of IEGT. Generally speaking, if the turnoff speed is too high, the overvoltage will cause the breakdown of the device. However, if the turnoff speed is too slow, it will increase loss and cause the device to overheat. Overvoltage in the switch will be limited by the MOV. So turnoff losses and turnoff peak power are major problem. As shown in Fig. 13.10, the turnoff process of different gate resistors is tested under the same current. It can be seen that as the gate resistance increases, the turnoff power decreases, but the loss increases. A relatively moderate value (33Ω) was finally chosen based on the maximum instantaneous power provided by the equipment manufacturer and the temperature threshold in actual operation.

Fig. 13.11 25 kA Test of parallel IEGTs



The results of 25 kA test are shown in Fig. 13.11. Although the structure has been as symmetrical as possible, the current is still unbalanced slightly between the two IEGTs at on-state. However, since independent resistors are used to connect to gate and cathode to suppress the circulating current, the turnoff process of two IEGTs is very synchronous, which improves the turnoff reliability.

4.3 Design of the Overall Modular-Designed Solid-State Switches

After completing the design of a single solid-state switch, it is necessary to further connect the modules in series to form overall power electronic multilevel series switches. According to the engineering technical specification, the series modular-designed solid-state switches need to withstand the DC voltage which are 1.1 times higher than the rated DC voltage (535 kV) and the impulse voltage which are 1.38 times higher than the overvoltage (800 kV), considering 8% of the series modules is breakdown. Because the parallel MOV is designed to be discrete, there is no need to calculate the unbalance factor between solid-state switches. The total voltage level is calculated by the series module. The rated voltage and maximum overvoltage of a modular solid-state switch are determined by the reference voltage $U_{ref} = 2.4$ kV and residual voltage $U_{res} = 4$ kV of the MOV connected in parallel. The final number of series modules is 320. The margins for DC and impulse voltages are 23% and 14%, respectively, which can meet the design requirement.

Because the energy of the 535 kV flexible DC system is very large, the circuit breaker requires the MOV to absorb energy more than 100 MJ. If only the discrete MOV design is adopted, each MOV needs to absorb energy more than 300 kJ, which will increase not only the volume of every module but also the cost of package of MOV. Additionally, the series redundancy of modular solid-state switches can create the overvoltage which exceeds 800 kV when all switches are working normally, potentially stressing other equipment.

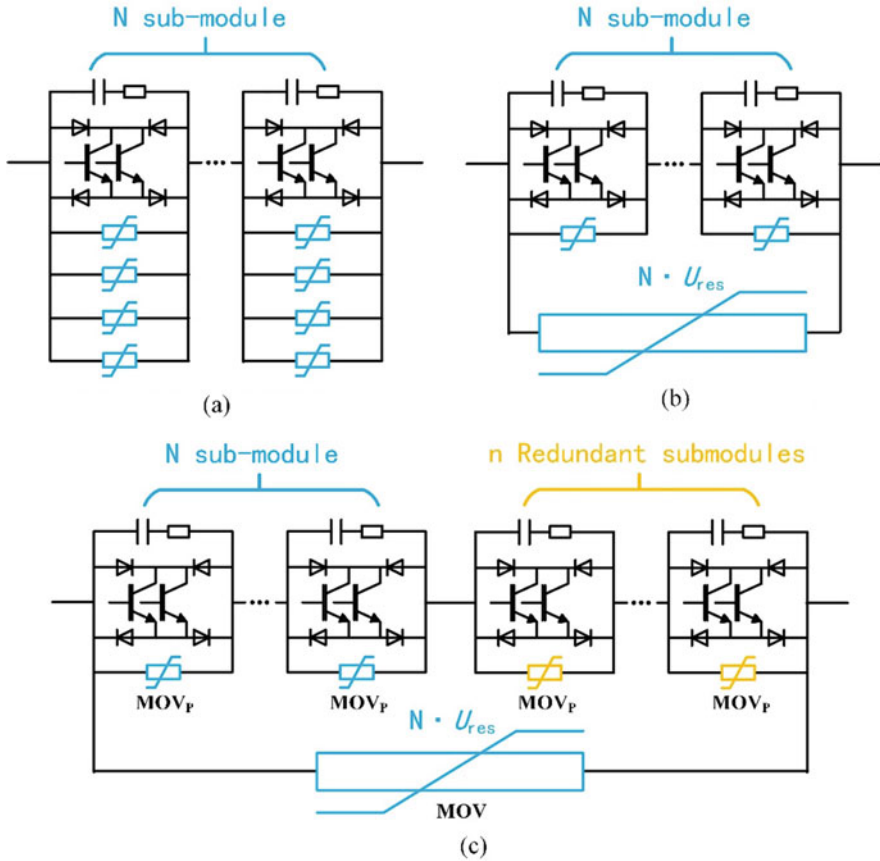


Fig. 13.12 MOV hierarchical design. (a) Original discrete MOV design. (b) Partial MOV integration. (c) Redundant modules added to maintain out-of-voltage characteristics

So, MOV is designed in layers, as shown in Fig. 13.12b, c. Original N sub-modules meet the overvoltage requirements. Then a lumped MOV is parallel to the series modular-designed solid-state switch valve to replace most of the MOV_s in the sub-modules, which not only meets the series voltage equalization requirements but also reduces the number of parallel MOVs in each module. To meet the voltage level and increase reliability, add the redundant modules as shown in Fig. 13.12c. The redundant modules are connected in series with the original N modules. Through hierarchical design, the functions of voltage-limiting protection and energy absorption of the original MOV are separated. In order to distinguish these two kinds of MOVs, the MOVs connected in parallel in the module are called protection MOV_p , and the MOVs connected in parallel with the overall solid-state switch valve are called energy absorption MOVs.

4.4 Experimental Verification

Eight modular-designed solid-state switch modules are integrated into a valve section, as shown in Fig. 13.13. Each module is only equipped with an MOV_p to limit overvoltage. Then the valve section is arranged as a valve tower. Each valve section will undergo a 25 kA shutoff test for component integrity after press-fitting, with typical waveforms shown in Fig. 13.14. It can be seen that the valve section is successfully turned off by 25 kA. Although there are some inconsistencies in the establishment of voltage of each module, they are all limited by their respective MOV_p after reaching the highest voltage.

To verify the effectiveness of the hierarchical design of MOV, a group of energy-absorbing MOV_s with a residual voltage of 160 kV were connected in parallel to 64 modules. A 25 kA turnoff test was performed on them. The result is shown in Fig. 13.15. After the IEGT is turned off, the current first strikes the MOV_p . Then the current is quickly transferred to the energy-absorbing MOV. The speed of the current transfer depends on the stray inductance of the circuit. During the entire breaking process, the overvoltage has been below 160 kV. Although the overall energy is not high due to the experimental conditions, it can be seen that the energy-absorbing MOV will absorb most of the energy, while MOV_p will only absorb the energy in the stray inductance on the branch of the solid-state switch.

Fig. 13.13 Actual diagram of solid-state switch valve section

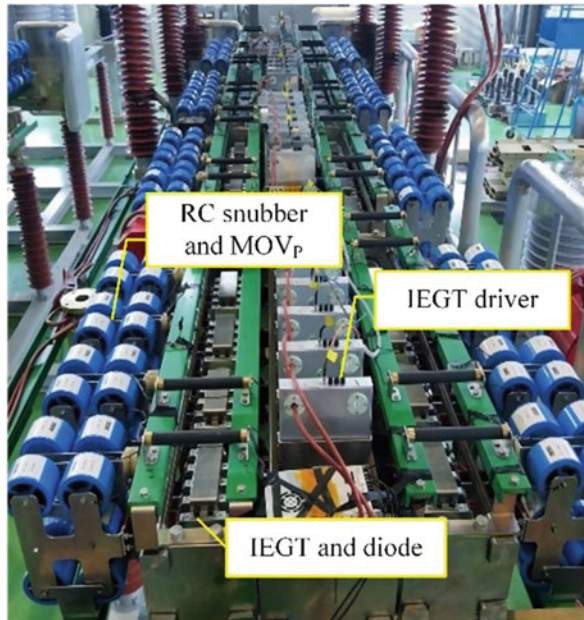


Fig. 13.14 Eight-series modules shut down 25 kA test

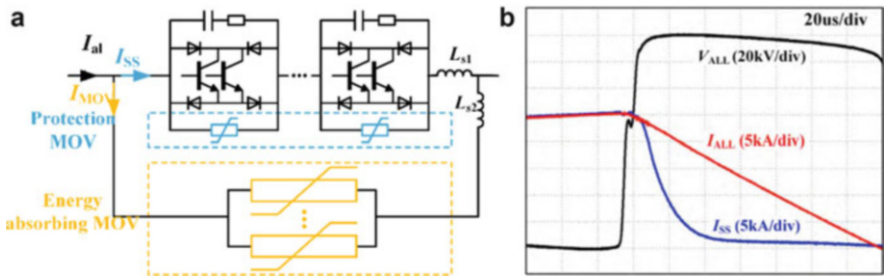
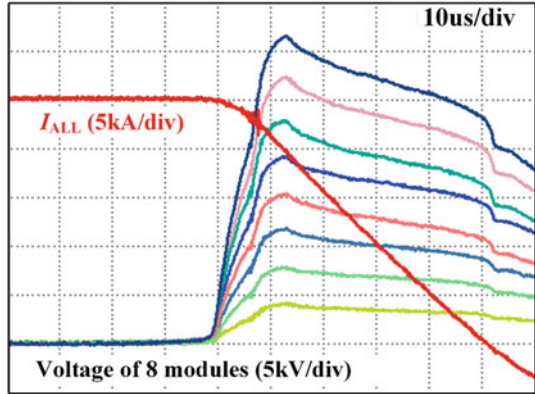


Fig. 13.15 (a) Test circuit and (b) waveform result

5 Design and Development of Current Commutation Device Circuit

The CCDC is used to commutate the current from the mechanical switch branch to the solid-state switch branch, which is the core equipment for the HCB to transition from the steady state to the transient state. It is the core equipment for transitioning the hybrid circuit breaker from steady state to dynamic. As depicted in Fig. 13.16, the CCDC consists of a transformer, a precharged capacitor C_D , and a pulse-closing switch based on thyristors. When the thyristors are turned on, the C_D will discharge through the transformer’s winding, thereby inducing a corresponding voltage on the winding of the other side. At this time, the MS is in the arcing state after the contact is separated, and the SS is in the on-state. Therefore, the CCDC can generate an oscillating circulating current between the MS and the SS to realize the transfer of current. It should be noted that both the CCDC and other components of the HCB, including the mechanical switch branch and the solid-state switch modules, need a high-voltage isolated power supply to work.

The C_d is continuously charged by a controllable power supply to keep its voltage at the required level, and the precharge is only used for a one-shot operation. When a fault occurs, the CCDC only operates once in the first breaking action of the HCB to

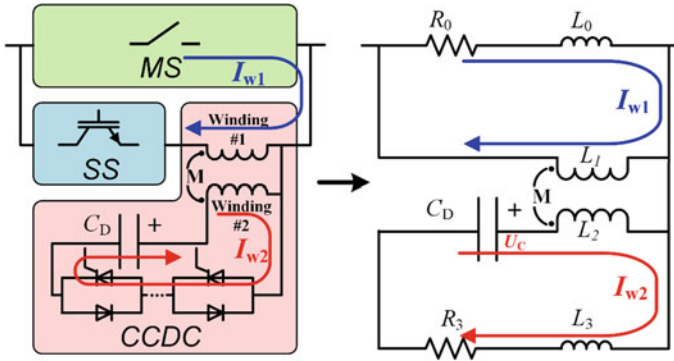


Fig. 13.16 Commutation principle of coupling negative voltage device

commutate the current from the mechanical switch branch to the solid-state switch branch. In the subsequent reclosure operation of the HCB, whether or not there is a fault, the commutation function of the CCDC is no longer needed. After the HCB completed the breaking and reclosing action, it will lock for a period of time, during which the energy storage capacitor of the CCDC will be recharged and the cooling time of the MOV will also be given.

The research team from Tsinghua University has carried out a detailed study on the parameter optimization method of the CCDC. The parameters of coupling negative voltage of the 535 kV DC circuit breaker needs to match the commutation current of 25 kA and the circuit parameters of the DC circuit breaker. As shown in Fig. 13.16, the air core transformer can be equivalent to L_1 , L_2 , and mutual inductance M . The arc voltage of MS is relatively low and can be ignored. Therefore, the commutation circuit composed of MS and SS can be simplified as RL circuit (R_0 and L_0). Likewise, the RL circuit on the CCDC's side can also be equivalent to R_3 and L_3 . Therefore, the circuit equation during commutation is:

$$\begin{cases} (L_0 + L_1) \frac{di_{\omega 1}}{dt} - M \frac{di_{\omega 2}}{dt} + R_0 i_{\omega 1} = 0 \\ (L_2 + L_3) \frac{di_{\omega 2}}{dt} - M \frac{di_{\omega 1}}{dt} + R_3 i_{\omega 2} = u_c \\ i_{\omega 2} = -C_D \frac{du_c}{dt} \end{cases} \quad (13.1)$$

Therefore, the expression of the commutation current component $i_{\omega 1}$ in the MS and the SS can be written as:

$$i_{\omega 1}(t) = A \cdot e^{-\sigma_1 t} + B \cdot e^{-\sigma_2 t} \sin(\omega t + \varphi) \quad (13.2)$$

Next, it is necessary to obtain R_0 , L_0 , R_3 , and L_3 as accurate as possible through experiments or simulations. Among them, the stray inductance L_0 of the MS of the circuit breaker and the SS has the greatest impact on the results. At the same time, because the inductance is related to the structure, it can only be obtained through

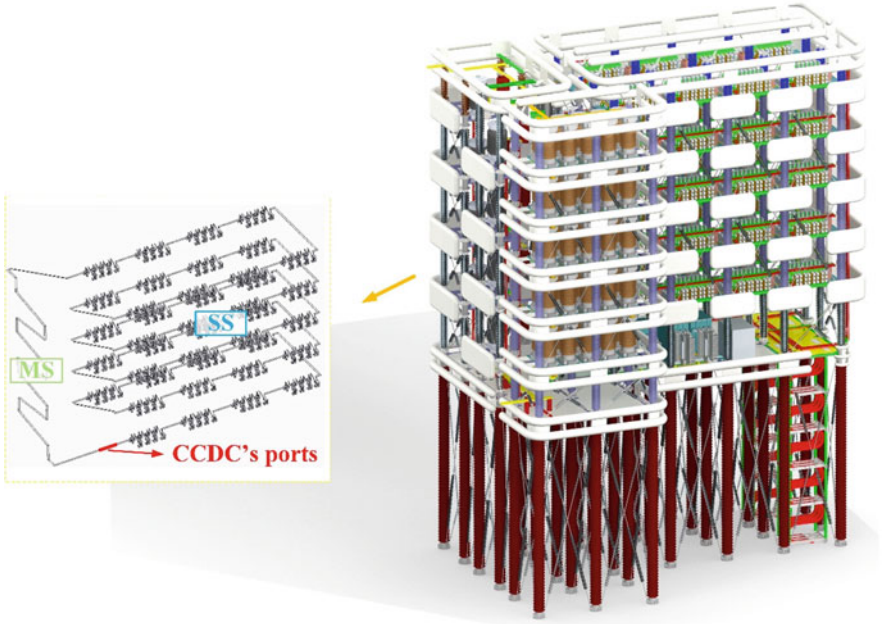


Fig. 13.17 Simulation of stray inductance of circuit breaker structure

structural simulation before the assembling of the circuit breaker. As shown in Fig. 13.17, the current path of the MS and the SS is modeled, and the simulation result of the structural stray inductance is $L_0 = 247 \mu\text{H}$.

The positive and negative peaks of i_{w1} need to reach 25 kA, then a series of solutions can be obtained by solving Eqs. (13.1) and (13.2). At this time, given a set of values of C_D and L_1 , the current capability i_{w2} and precharging voltage U_C required by the corresponding CCDC can be obtained. This gives the cost of CCDC. Among them, the cost of the capacitor is linearly related to its energy, the cost of the thyristor is related to the number of series and parallel connection, and the cost of the charging device is linearly related to the voltage:

$$\begin{cases} \text{Cost of Capacity} = K_1 \cdot C_D U_C^2 \\ \text{Cost} = K_2 \cdot \text{ceil}\left(\frac{U_C}{U_T}\right) \cdot \text{ceil}\left(\frac{i_{w2}}{I_T}\right) \\ \text{Cost of Precharge Device} = K_3 \cdot U_C \end{cases}$$

Finally, the total cost is optimized: the energy storage capacitor $C_D = 650 \mu\text{F}$, and transformer parameters $L_1 = 257.5 \mu\text{H}$, $L_2 = 44.3 \mu\text{H}$, and $M = 104.9 \mu\text{H}$ are finally determined.

Figure 13.18 shows the real CCDC and the equivalent load test waveform. The coupling transformer adopts an ironless air core to avoid saturation at high

Fig. 13.18 Real product of CCDC

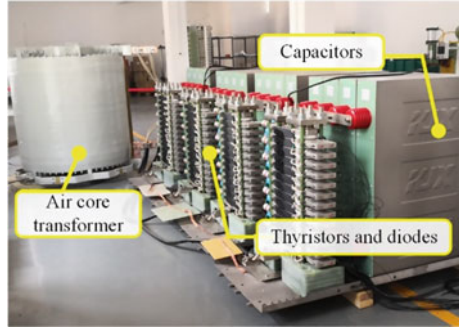
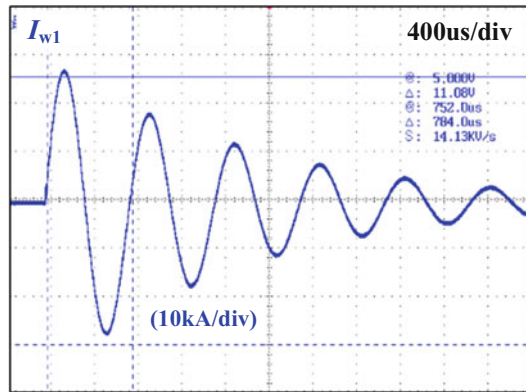


Fig. 13.19 Equivalent load test waveform



current. Capacitor and thyristor switches are divided into four parallel modules for high-current capability. Because the current generated by the CCDC needs to cooperate with the actual MS and the SS, the equivalent impedance is used for the commutation test at that time. Test results show that the CCDC can generate the required positive and negative current peaks (>25 kA) within 0.6 ms (Fig. 13.19).

6 Integration of DC Circuit Breaker and Multipotential High-Voltage Isolation Power Supply System

Figure 13.20 shows the connection diagram of the 535 kV DC circuit breaker. First, 8 MSs are connected in series (the voltage-equalizing circuit is omitted in the figure) to form the current-conducting branch of the DC circuit breaker. The SS is divided into five layers, each layer of the SS includes 64 sub-modules, and the energy-absorbing MOV is also divided into five layers in parallel with the corresponding layer of the SS. The layered design is mainly considered from the structural insulation. Because the number of redundant modules is large, if the damaged locations of the modules are concentrated in the same area, the original

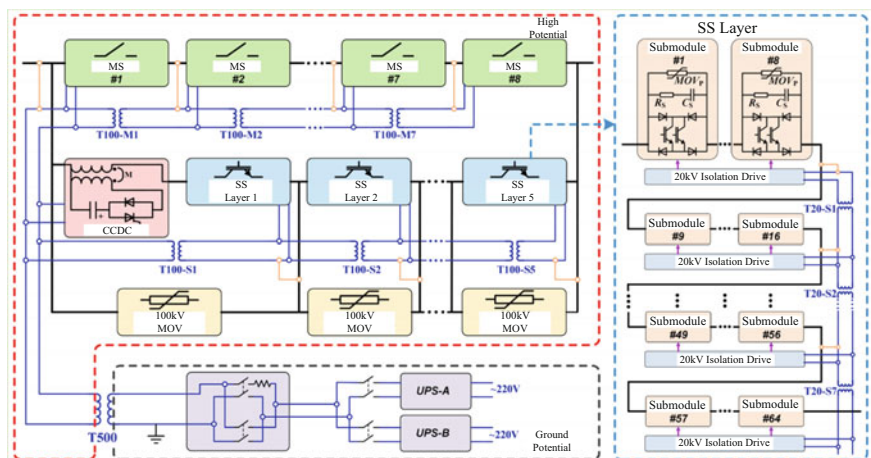


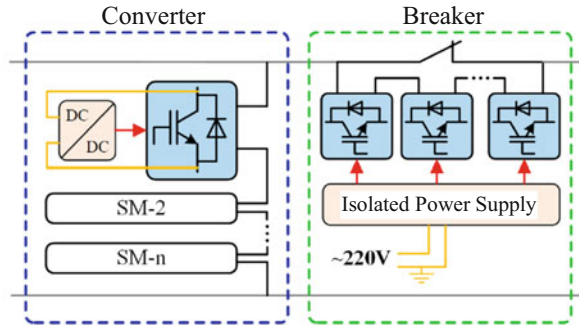
Fig. 13.20 535 kV DC circuit breaker connection diagram

potential distribution of the circuit breaker will be greatly changed, increasing the difficulty of the corresponding insulation design. After the layered design is adopted, the maximum insulation level between the layers is given. The SS part is firstly designed by standard of the 100 kV rating and then stacked to become a 535 kV SS. It should be pointed out that after layering, the redundant modules of each layer are no longer shared. So when the loss of any layer of modules exceeds the design value, the entire breaker needs to be shut down. The CCDC is special. It is connected in series with the first layer of SS and then in parallel with the first layer of energy-absorbing MOVs. Because the CCDC can be placed at any position of the MS and the SS circuit, it will not affect the commutation. In addition, when the SS is turned off, the CCDC is only equivalent to an inductance of the order of 100 μ H, which will not bring additional effects.

In general, the integrated design idea for 535 kV DC circuit breaker is to connect low-voltage-level devices in series. After using the modular series technology, the increase of the voltage level of the circuit breaker will not cause other technical problems. But there is another problem that will gradually become prominent as the voltage increases, that is, the problem of high-voltage isolated power supply.

In fact, the operating conditions of DC circuit breaker are very special for high-voltage power electronic equipment, which bring great difficulties to the power supply system. As shown in Fig. 13.21, the power electronic modules in the converter will withstand a certain voltage during operation, so the device can directly obtain energy from the potential difference by the DC-DC power supply. Or in some other applications where it is difficult to find a stable potential difference, the energy can be acquired from the line by electromagnetic induction through the alternating current in the device. In contrast, DC circuit breakers can be regards as a small resistance in the normal state. The voltage of power electronic devices is almost 0V. At the same time, energy cannot be obtained from the current in the

Fig. 13.21 Comparison of power supply mode between converter and DC circuit breaker



DC line. So, the DC circuit breaker can only obtain the energy from the external distribution network and then supplies for the electrical equipment through the isolated power supply system.

The 535 kV circuit breaker contains a large number of electrical equipment; each SS module, each MS, and the CCDC need to be powered; and these devices are not on the same potential, which brings huge difficulties to the isolated power supply. Hence, a multipotential high-voltage isolation power supply system needs to be specially designed for the 535 kV DC circuit breaker. The main structure of the isolated power supply system has been given in Fig. 13.20.

Firstly, the components of the DC circuit breaker are actually at the same high potential when it is in the closing state. However, the DCCB needs to withstand the transient overvoltage and the bus voltage during the transient breaking process; thus, the potentials of the series modules are inconsistent. So a 535 kV isolation transformer (T500) is used to take 220 V alternating voltage from the ground to the high potential and provides a power supply port for the DC circuit breaker at the same potential as the high-voltage line.

Secondly, the 100 kV isolation transformer (T100) is used in cascade form to provide power supply ports with different potentials for five layers of SS and 8 MS. It should be noted that the isolation transformers (T100-M1 to T100-M7) for the 7 MS and the isolation transformers (T100-S1 to T100-S5) for the 5 SS both withstand 535 kV terminal voltage of DC circuit breaker. Because the SS adopts a layered design, the isolation transformers can be directly connected to each layer of 100 kV MOV in an equipotential connection after they are cascaded, and there is no need to consider the problem of voltage equalization. However, there is no MOV in parallel with the MS but the static balancing resistor and the dynamic balancing RC circuit in parallel with the MS, so the isolation level needs to be relatively high. In order to unify the specifications in the project, the same 100 kV isolation transformer is adopted here. In addition, the same idea is used inside the SS, and the 20 kV isolation transformers are used for the cascaded power supply (T20-S1 ~ T2-S5) for the valve section (includes eight modules). Figure 13.22 shows the physical map of 535 kV, 100 kV, and 20 kV isolation transformers, and the specific parameters are given in Table 13.2.



Fig. 13.22 Physical drawing of isolation transformer. (a) 500 kV isolated transformer. (b) 100 kV isolated transformer. (c) 20 kV isolated transformer

Table 13.2 Parameters of isolation transformers

Parameter	500 kV isolated Transformer T500	100 kV isolated Transformer T100	20 kV isolated Transformer T20
Operating range	190 to 250 V AC, 45 to 65 Hz		
DC withstand voltage	588 kV	110 kV	20 kV
Short-time DC withstand voltage (1 min)	856 kV	179 kV	35 kV
Peak of switching impulse withstand voltage	1292 kV	193 kV	45 kV
Peak of lightning impulse withstand voltage	1425 kV	233 kV	50 kV

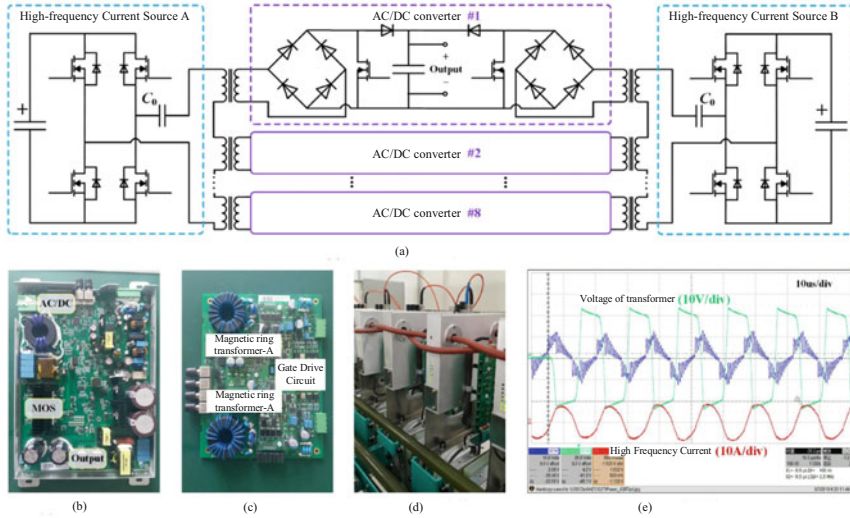


Fig. 13.23 Double-redundancy high-frequency isolation energy supply method based on magnetic ring. (a) Principle of dual redundancy high-frequency isolation power supply unit. (b) High-frequency current source. (c) Energy acquisition module. (d) Insulated cables. (e) Typical waveform

So far, 220 V AC power can be supplied to each valve section, and a high-frequency isolation power supply unit based on magnetic ring is used inside the valve section, which can directly provide isolated power for eight modules. First, a high-frequency current source is used to generate a resonant current of about 60 kHz, and then an insulated cable is used to make the current pass through the magnetic ring transformer of the drive board in each module, and the corresponding AC voltage is induced on the secondary side of the transformer. After rectification and stabilization, it can be used for IEGT gate driver. As shown in Fig. 13.23, both the high-frequency current source and the magnetic ring energy acquisition module adopt double redundancy, which can ensure continuous working when any part fails.

7 Experimental Research of the Whole DC Circuit Breaker

Figure 13.24 shows the experimental circuit and control sequence of the interruption platform for the 535 kV DC circuit breaker. In order to test the reclosing function of the DC circuit breaker, the experimental platform is equipped with two independent discharge capacitors. Among them, C_{DC1} is used to generate a fault current of 25 kA, and C_{DC2} with a smaller capacitance is used to simulate the situation that the system fault is not cleared during reclosing.

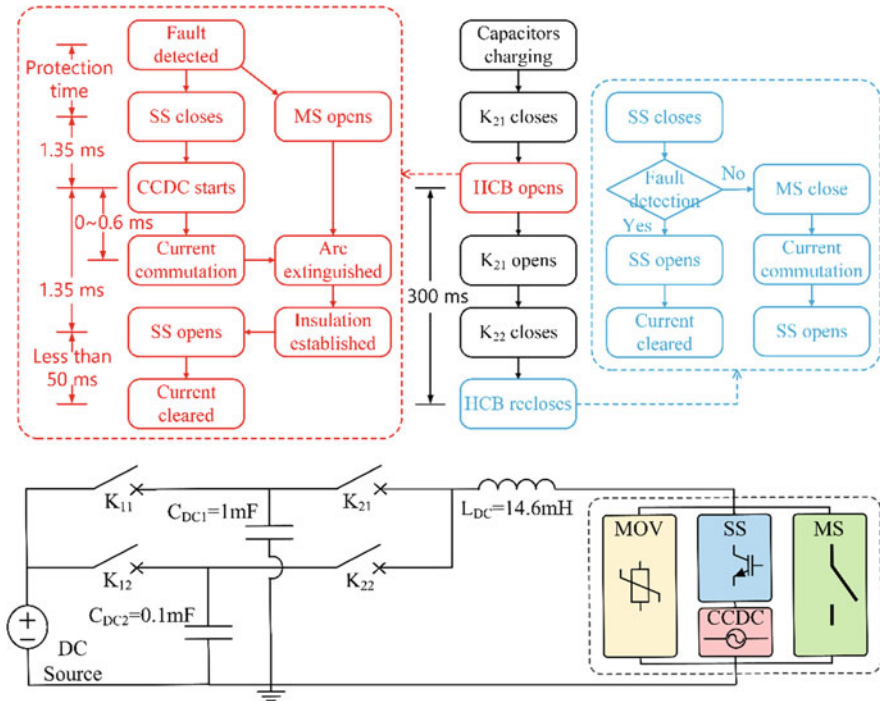


Fig. 13.24 Schematic diagram of experimental circuit and control flow of DC circuit breaker

The overall experimental process is as follows: the DC circuit breaker is initially in the closed state, and the two groups of capacitors are charged separately under the control of K_{11} and K_{12} . At the beginning of the experiment, K_{21} is closed, and C_{DC1} discharges the inductor L_{DC} . When the protection device detects the fault current, it sends a breaking command to the DC circuit breaker. The DC circuit breaker will trigger the MS, the SS, and the CCDC successively through the preset action sequence and finally clear the fault. After the current is completely removed, the circuit breaker is in the blocking state. At this time, K_{21} is opened, and K_{22} is then closed. After that, the controller will send a reclosing command to the DC circuit breaker. The circuit breaker will first turn off the SS and observe the current rise to determine whether there is a fault. If the current is not too large, the MS will be closed. Because the voltage drop of the MS is lower than that of the SS, the current will be automatically commutated to the MS, and the SS will resume blocking state after a period of time. Otherwise, if the current is too large, the SS will directly turn off and clear the fault. Figures 13.25 and 13.26 shows the practical photograph of the experimental platform and DC circuit breaker.

Before the final breaking experiment, a 25 kA current turnoff experiment test was performed on the integrated SS to verify the reliability of the centralized operation of 320-series modules. The test results are shown in Fig. 13.27. The results show

Fig. 13.25 High-current experimental platform

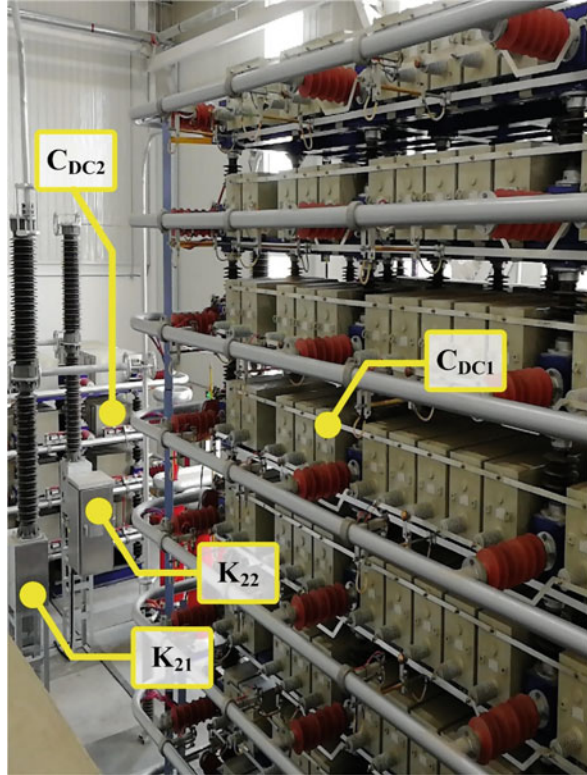


Fig. 13.26 Practical photograph of circuit breaker

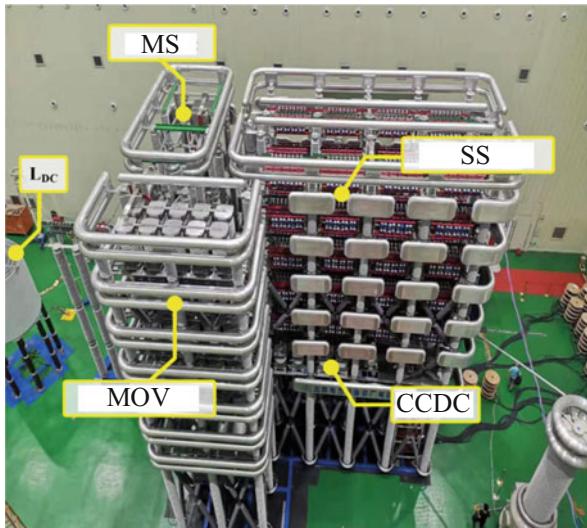
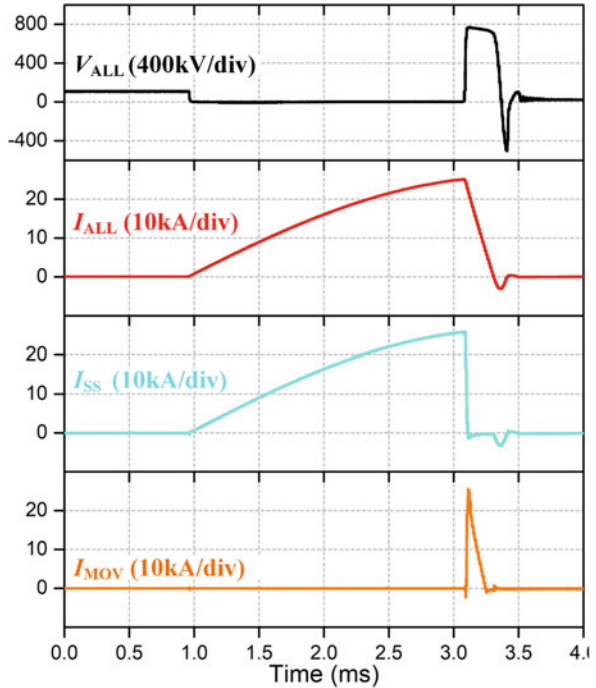


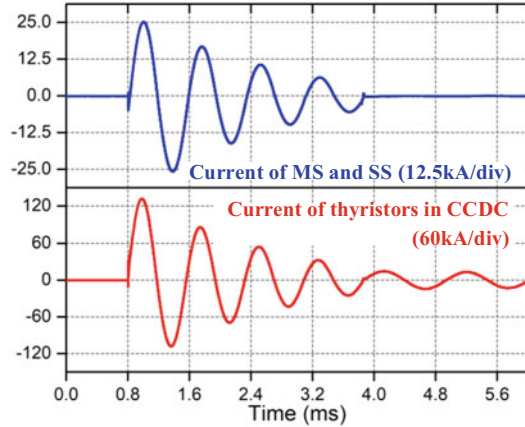
Fig. 13.27 25 kA turnoff test of the integrated SS



that the integrated SS can successfully turn off the current of 25 kA, and the energy absorption MOV limits the overvoltage to less than 800 kV at 25 kA. Because the terminal has withstood an operating impulse voltage of 800 kV, the experiment also examines the insulation between the terminals of the mechanical structure and the stability of the isolated power supply system.

Since only the estimated equivalent load is used to verify the commutation capability of the CCDC in Sect. 3, it is necessary to retest the CCDC in actual MS and SS. The thyristor in the CCDC is triggered when both the MS and the SS are in a conducting state. The actual measured current in the SS and the thyristor is shown in Fig. 13.28. The CCDC successfully generated an oscillating current of 25 kA between the MS and the SS. The first oscillation period is 0.8 ms, indicating that the calculation of stray inductance is roughly accurate. However, because of the existence of the voltage drop of the device in the SS, the equivalent resistance of the SS is larger when the current is smaller, so the amplitudes of current in the subsequent oscillation periods are different from those used equivalent load previously. At 3.8 ms, because the voltage generated by the CCDC is no longer enough to cover the turn-on voltage drop of all devices, the current in the SS completely stops oscillating. But in fact, only the first two peaks of current affect the commutation capability of the CCDC, so it is only required to pay attention to whether the peaks at 0.2 ms and 0.6 ms can reach 25 kA.

Fig. 13.28 Test of practical load commutation capacity of CCDC



After verifying that all components have reached the expected performance, the current breaking and reclosing test of the circuit breaker was carried out as shown in Fig. 13.29. Because of the asymmetry of current of CCDC, both forward and reverse current tests are required. The results are shown in Fig. 13.29, respectively. The experimental platform needs to charge C_{DC1} to 115 kV to generate 25 kA and then discharge the circuit through K_{21} . It can be seen that after the DC circuit breaker receives the breaking command, the MS starts to open first, but the current of the MS continues to rise because the vacuum arc voltage is very low. After 1.35 ms, the CCDC is triggered and causes an oscillating current in the MS and the SS. During the forward current breaking process (Fig. 13.29 left), the initial direction of the oscillating current is the direction which commutation requires, so the MS current directly drops to zero. In the reverse current breaking process (Fig. 13.29 right), the initial direction of the oscillating current is opposite to the direction of commutation, so the MS current first increases and then decreases, and before the second oscillation peak, it drops to zero. Because the SS is in the conducting state at this time, once the current of the MS crosses zero, the arc will be extinguished directly. After that, the SS continues to carry the fault current. Finally, at 2.7 ms after the command is received, the MS contacts are sufficiently spaced, and the SS is turned off, resulting in an overvoltage of 800 kV to rapidly decay the current, and the breaking is completed.

Figure 13.30 shows the test results of the reclose. After the DC circuit breaker completes the first 25 kA current interruption, K_{21} is opened, and K_{22} is closed to connect C_{DC2} to the experimental circuit to simulate the pre-fault in the system. After 300 ms, the DC circuit breaker tries to reclose through its SS and turns off again quickly when the current rises to 6.8 kA.

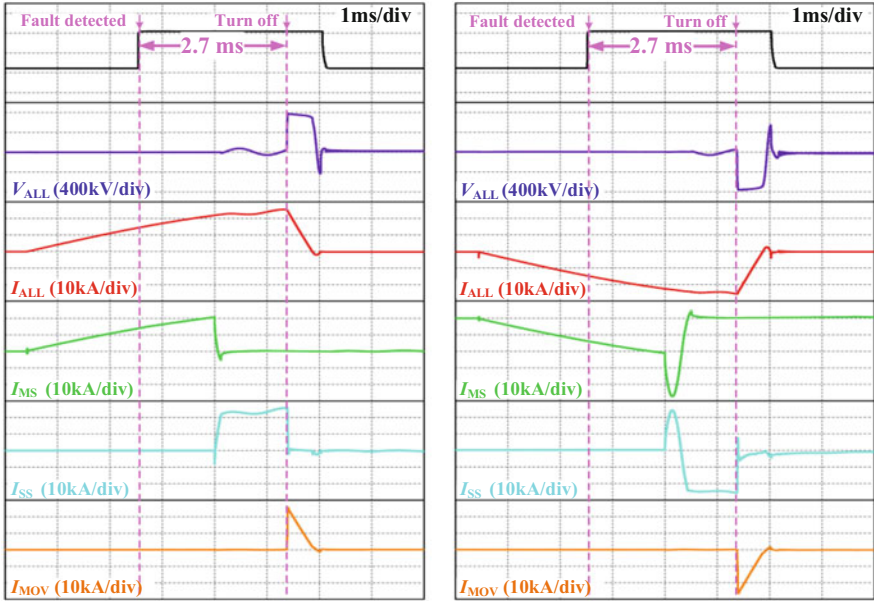


Fig. 13.29 DC circuit breaker current shutdown test waveform

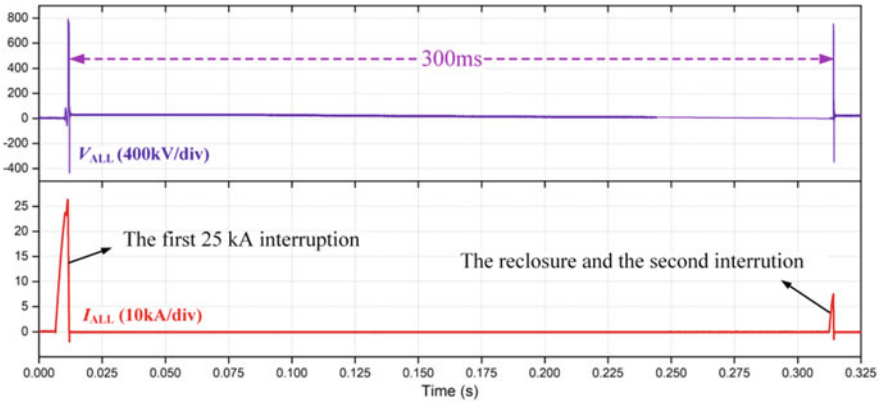


Fig. 13.30 Opening and reclosing test waveform

8 Concluding Remarks

In this chapter, the engineering application research of 535 kV hybrid DC circuit breaker is carried out:

1. A 535 kV/25 kA power electronic multilevel switch is developed based on the discrete MOV modular connection and the diode bridge bidirectional optimized



Fig. 13.31 535 kV DC circuit breaker in the Kangbanuoer converter station

structure. IEGT and ordinary recovery diodes are successfully applied to the field of DC circuit breakers for the first time. On the basis of the research, the fast MS and the current commutation driver circuit suitable for 535 kV DC circuit breaker are developed, respectively.

2. A dedicated multipotential high-voltage isolation power supply system is also designed for large-scale electrical equipment in DC circuit breakers. Two experimental platforms for power electronic series devices and hybrid DC circuit breakers are built to realize interruption testing of DC circuit breaker. It has been proven by experiments that the 535 kV hybrid DC circuit breaker can interrupt a current of 25 kA within 2.7 ms and withstand 800 kV overvoltage during the breaking process, reaching the world's leading level.
3. At present, two 535 kV hybrid DC circuit breakers based on the scheme in this chapter have completed all installation and commissioning in the Kangbanuoer converter station of Zhangbei Flexible DC Project (Fig. 13.31) and have been put into official operation.

References

1. G. Tang et al., Research on key technology and equipment for Zhangbei 500kVDC grid. [J] *High Volt. Eng.* **44**(07), 2097–2106 (2018). <https://doi.org/10.13336/j.1003-6520.hve.20180628001>
2. W. Chen, R. Zeng, J. He, Y. Wu, X. Wei, T. Fang, Z. Yu, Z. Yuan, Y. Wu, W. Zhou, B. Yang, L. Qu, Development and prospect of direct-current circuit breaker in China. *High Volt.* **6**, 1–15 (2021). <https://doi.org/10.1049/hve2.12077>
3. X. Zhang et al., A state-of-the-art 500-kV hybrid circuit breaker for a dc grid: The world's largest capacity high-voltage dc circuit breaker. *IEEE Ind. Electron. Mag.* **14**(2), 15–27 (2020). <https://doi.org/10.1109/MIE.2019.2959076>

4. J. Wen, *Research on Current Commutation and Dielectric Recovery Characteristics of the Ultra-Fast Mechanical Switch in DC Circuit Breaker* (Tsinghua University, [D] Beijing, 2017)
5. J.-F. Chen, J.-N. Lin, T.-H. Ai, The techniques of the serial and paralleled IGBTs, in *Proceedings of the 1996 IEEE IECON. 22nd International Conference on Industrial Electronics, Control, and Instrumentation*, vol. 2, (1996), pp. 999–1004. <https://doi.org/10.1109/IECON.1996.566015>
6. X. Zhang, Z. Yu, Z. Chen, B. Zhao, R. Zeng, Optimal design of diode-bridge bidirectional solid-state switch using standard recovery diodes for 500-kV high-voltage DC breaker. *IEEE Trans. Power Electron.* **35**(2), 1165–1170 (2020). <https://doi.org/10.1109/TPEL.2019.2930739>
7. W. Wen, Y. Huang, T. Cheng, et al., Research on a current commutation drive circuit for hybrid dc circuit breaker and its optimization design [J]. *IET Gener. Transm. Distrib.* **10**(13), 31193126 (2016)
8. X. Zhang, Z. Yu, R. Zeng, M. Zhang, Y. Zhang, F. Xiao, W. Li, HV isolated power supply system for complex multiple electrical potential equipment in 500 kV hybrid DC breaker. *High Volt.* **5**, 425–433 (2020). <https://doi.org/10.1049/hve.2019.0260>
9. M. Liserre, T. Sauter, J.Y. Hung, Future energy systems: Integrating renewable energy sources into the smart power grid through industrial electronics. *IEEE Ind. Electron. Mag.* **4**(1), 18–37 (2010). <https://doi.org/10.1109/MIE.2010.935861>
10. R. Zeng et al., A prospective look on research and application of DC power distribution technology. *Proc. CSEE.* **38**(23), 6791–6801 (2018). (in Chinese)
11. J. Hafner, Proactive hybrid HVDC breakers-A key innovation for reliable HVDC grids, in *Proc. CIGRE Bologna Symp.*, (2011), pp. 1–8
12. J. Magnusson, R. Saers, L. Liljestr and, et al., Separation of the energy absorption and overvoltage protection in solidstate breakers by the use of parallel varistors [J]. *IEEE Trans. Power Electron.* **29**(6), 27152722 (2014)
13. J. Hu, *Research of ZnO Varistor with High Voltage Gradient Applied in Ultrahigh Voltage Arrester [D]* (Tsinghua University, Beijing, 2008)
14. W. Wen, Y. Huang, M. Al Dweikat, et al., Research on operating mechanism for ultrafast 40.5kv vacuum switches [J]. *IEEE Trans. Power Deliv.* **30**(6), 25532560 (2015)
15. Z. Chen et al., Analysis and experiments for IGBT, IEGT, and IGCT in hybrid DC circuit breaker. *IEEE Trans. Ind. Electron.* **65**(4), 2883–2892 (2018). <https://doi.org/10.1109/TIE.2017.2764863>
16. Toshiba ST3000GXH24A Datasheet (2020)